DOI:
10.1021/acs.jpclett.0c03574

New Insights into Secondary Organic Aerosol Formation: Water Binding to Limonene

*S. Indira Murugachandran, Jackson Tang, Isabel Peña†, Donatella Loru‡, M. Eugenia Sanz**

Department of Chemistry, King's College London, London SE1 1DB, UK

[†] Present Address: Departamento de Química Física y Química Inorgánica, Universidad de Valladolid, E-47011 Valladolid, Spain.

[‡] Present Address: Deutsches Elektronen-Synchrotron (DESY), Notkestraße 85, Geb. 25f / Office 354, D-22607 Hamburg.

AUTHOR INFORMATION

Corresponding Author

* E-mail: maria.sanz@kcl.ac.uk

ABSTRACT. Limonene is an abundant monoterpene in the atmosphere and one of the main precursors of secondary organic aerosol. Understanding its interactions with atmospheric molecules is crucial to explain aerosol formation and the various products obtained from competing reaction pathways. Here, using broadband rotational spectroscopy in combination with computational calculations, we show that limonene effectively interacts with water forming a variety of complexes. Seven different isomers of limonene-H_2O, where water and limonene are

connected by O–H···π and C–H···O interactions, have been unambiguously identified. Water has been found to preferentially bind to the endocyclic double bond of limonene. Our findings demonstrate a striking ability of water to attach to limonene, and enrich our knowledge on the possible interactions of limonene in the atmosphere.

TOC GRAPHICS

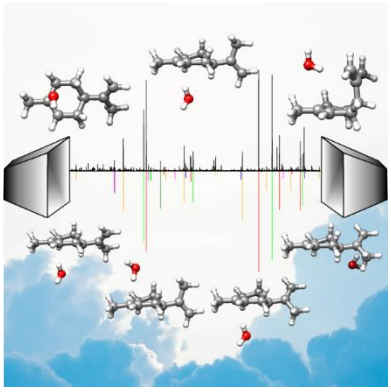

Non-covalent interactions • Rotational spectroscopy • Hydrogen bond • Structural analysis • Microsolvation.

Secondary organic aerosol (SOA) is one of the largest sources of uncertainty in climate modelling as its composition, formation and evolution are not well understood.[1–3] SOA is formed from oxidation reactions of volatile organic compounds (VOCs) in the atmosphere[3] and their condensation into aerosol phase. However, critical information on how molecules interact with each other and start forming clusters is missing. In particular, the role of water is not clear[4]. Water is abundant in the troposphere, and therefore it can compete with atmospheric oxidants for

binding to VOCs. Water can also influence the evolution of oxidation products and the formation of low volatility species, eventually changing the composition and yield of SOA[3,5–7]. In addition, water has been reported to change reaction barrier heights upon complex formation,[8] therefore having a catalytic or inhibitory effect with important consequences for atmospheric reactions[9].

The major contributors to SOA formation are monoterpenes,[1,10] a class of compounds with molecular formula $C_{10}H_{16}$ produced by plants. Monoterpenes are released in large quantities to the atmosphere, where they react with OH and NO_3 radicals, and ozone, forming other compounds that could undergo further chemical reactions and eventually aggregate to produce SOA.[3] Relative humidity plays a significant role in SOA formation from monoterpene oxidation processes[5–7,11]but the effect of water differs depending on whether the monoterpene has an endocyclic or exocyclic bond, the relative humidity and the oxidant. To improve our understanding on the effect water has on the mechanism of SOA production it is necessary to know how monoterpenes start interacting with water at the molecular level. Rotational spectroscopy is a fitting tool for these studies since it yields very precise structural information in the gas phase, being able to distinguish between subtly different configurations of the interacting molecules without ambiguity. It has been applied in a few studies of water binding to Criegee intermediates[12], and to ketones and aldehydes that are products of monoterpene atmospheric oxidation[13–17]. However, to our knowledge there are no studies addressing water binding to non-oxidised monoterpenes that are SOA precursors.

In this work, we present the investigation of the interactions of the monoterpene limonene with water using broadband rotational spectroscopy in combination with quantum chemical calculations. Limonene is one of the most abundant monoterpenes in nature and one of the main SOA precursors.[10] Limonene is composed of a cyclohexene ring with methyl and isopropenyl

substituents in para position (Fig. 1). Having both an exocyclic and an endocyclic double bond, limonene is an ideal candidate to explore whether there is any preferential binding of water to one or the other, and whether there are any differences in those interactions depending on the conformation adopted by limonene.

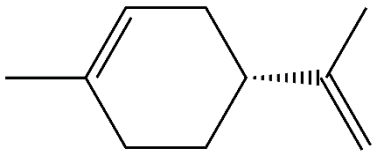

Figure 1. Molecular structure of (*R*)-(+)-limonene.

Limonene has six possible conformations, arising from the axial or equatorial position of the isopropenyl group and its rotation, as depicted in Fig. S1 (Supporting Information, SI). In the liquid phase, three equatorial conformers have been reported to be present by several vibrational spectroscopic methods (IR, Raman, and VCD[18]), and by NMR[19]. In the gas phase, rotational spectroscopy revealed the existence of four conformers, one axial and three equatorial, with two equatorial conformations being dominant[20,21]. For the study of limonene-H_2O, we considered all six possible conformations of limonene with different arrangements of the water molecule interacting with limonene double bonds (Fig. S2, SI), and predicted limonene-H_2O lower-energy isomers using B3LYP-D3BJ[22,23] and MP2 methods with the 6-311++G(d,p) basis set, within Gaussian 09[24] (Methods, SI). The isomers predicted within 12 kJ mol^{-1} of the global minimum (of a total of 30 isomers with energies up to 16.7 kJ mol^{-1}) are shown in Tables 1 and S1.

Table 1. Calculated spectroscopic parameters at different levels of theory of the fourteen lower-energy isomers of limonene-(H_2O). Observed isomers are in bold.

	B3LYP-D3BJ/6-311++G(d,p)			MP2/6-311++G(d,p)		
	A/*B*/*C*[a]	μ_a /μ_b/μ_c[b]	ΔE[c]	*A*/*B*/*C*[a]	μ_a /μ_b/μ_c[b]	ΔE[c]
EQA-3[d]	**1611.8/637.5/561.2**	**−1.7/0.7/0.7**	**0.0**	**1606.5/639.6/562.5**	**−1.6/0.7/0.7**	**0.0**
EQA-4	**1597.9/640.3/556.3**	**1.2/−1.3/1.2**	**0.8**	**1595.9/643.8/558.7**	**1.2/−1.0/1.2**	**0.6**
EQA-2	1644.7/596.9/499.6	−1.0/−1.0/−0.2	1.1	1591.7/614.8/512.8	−1.2/−0.8/−0.2	3.0
EQC-4	**1581.6/646.2/554.1**	**−1.6/0.2/1.2**	**1.3**	**1580.1/649.6/558.2**	**−1.6/0.1/1.2**	**1.9**
EQC-3β	**1643.6/599.3/551.7**	**−0.1/1.6/1.2**	**1.7**	**1652.7/600.9/549.1**	**0.0/1.5/1.2**	**2.4**
EQC-3α	1631.6/602.8/555.1	0.9/1.8/0.9	2.0	1627.9/606.2/555.4	1.1/1.7/0.8	2.8
AXa-3	1275.9/856.9/709.3	1.8/2.3/−0.2	2.5	1250.1/871.1/711.5	2.1/1.6/−0.2	3.0
EQA-1	1675.9/581.8/490.9	0.3/1.4/−0.8	2.5	1680.1/583.0/494.6	0.5/1.3/−0.9	4.1
EQa-4	**1595.7/614.9/577.6**	**−1.3/0.7/0.6**	**2.5**	**1594.5/614.9/577.6**	**−1.2/0.6/0.8**	**1.9**
AXa-4	1571.1/689.9/623.7	−0.2/−1.3/0.2	2.6	1556.1/703.9/641.6	−0.2/−1.4/0.3	0.4
EQC-2	**1635.7/599.3/502.3**	**−1.0/−1.0/−0.4**	**2.9**	**1613.2/612.9/524.1**	**−1.2/−0.2/−0.8**	**4.2**
EQa-3	1628.1/608.4/550.9	−1.2/−1.3/1.1	3.1	1624.2/612.4/551.8	−1.2/−1.2/1.1	2.8
AXa-2α	**1215.6/905.6/720.2**	**1.7/0.3/−0.4**	**3.6**	**1190.7/927.4/728.0**	**1.6/0.2/−0.6**	**2.3**

[a] *A*, *B* and *C* are the rotational constants in MHz. [b] μ_a, μ_b and μ_c are the values of the electric dipole moment components along the principal inertial axes in Debye. [c] Calculated relative zero-point corrected energies in kJ mol^{-1}. [d] Nomenclature of limonene conformers follows that of ref. [20], see SI; 1 and 2 indicate water interactions with the exocyclic double bond on its opposite sides; 3 and 4 indicate water interactions with the endocyclic double bond above and below the cyclohexene ring, respectively.

The theoretical predictions guided our search for limonene-H_2O isomers in the rotational spectrum, which was collected in the 2-8 GHz range using our chirped-pulse Fourier transform microwave spectrometer[25,26] (Methods, SI). Several species previously identified were observed in the dense spectrum, including the four gas-phase limonene conformers[20,21], as well as water hexamer, heptamer, nonamer and decamer complexes.[27–30] After all these transitions were removed, we identified seven different species of limonene-H_2O. Preliminary assignments were confirmed by fitting additional transitions using the semi-rigid rotor Hamiltonian of Watson in the A reduction and I^r representation[31] implemented in Pickett's programs.[32] The final experimental spectroscopic constants are presented in Table 2 and all measured transitions are collected in the SI (Tables S24-S53).

Table 2. Experimental spectroscopic parameters for the observed isomers of limonene-H_2O.

	Isomer 1 **EQA-3**	**Isomer 2** **EQA-4**	**Isomer 3** **EQC-4**	**Isomer 4** **EQC-2**	**Isomer 5** **EQa-4**	**Isomer 6** **EQC-3β**	**Isomer 7** **AXa-2α**
A[a] (MHz)	1579.68818(50)[b]	1570.50759(55)	1549.01064(76)	1609.5558(18)	1566.65(40)	1633.554(15)	1178.0127(64)
B (MHz)	633.69037(29)	634.6738 (23)	644.62745(41)	599.20896(40)	606.8071(11)	592.23314(51)	902.24692(86)
C (MHz)	553.80812(26)	548.86330(23)	549.91766(40)	506.86000(43)	570.29123(95)	543.81218(59)	703.91112(85)
Δ_J (kHz)	0.1061(36)	0.0788(27)	0.1026(51)	0.1094(52)	0.136(16)	0.1505(81)	0.166(20)
Δ_{JK} (kHz)	1.420(23)	1.155(28)	1.102(22)	0.633(88)	0.73(24)	0.983(85)	0.73(12)
δ_J (kHz)	0.0235(29)	0.0148(19)	0.0385(34)	-	-	-	-
a/b/c[c]	y/y/y	y/y/y	y/n/y	y/y/y	y/n/n	n/y/y	y/n/n
σ[d]	4.4	4.1	5.6	6.4	7.7	7.2	7.2
N[e]	58	61	45	30	15	26	15

[a] A, B and C are the rotational constants; Δ_J, Δ_{JK} and δ_J are the quartic centrifugal distortion constants. [b] Standard error in parentheses in the units of the last digit. [c] Yes (y) or no (n) observation of *a*-, *b*- and *c*-type transitions. [d] Rms deviation of the fit. [e] Number of rotational transitions included in the fit.

The observed isomers, 1 to 7, could be assigned to species **EQA-3**, **EQA-4**, **EQC-4**, **EQC-2**, **EQa-4**, **EQC-3β** and **AXa-2α**, respectively (Table 2) by first, comparing the experimental and theoretical rotational constants; and second, comparing the observed transitions and their relative intensities with the predicted dipole moment components (see further details in the SI). Further confirmation was obtained from the observation of their HOD, DOH, $H_2{}^{18}O$ and D_2O isotopologues at the predicted frequency shifts (Tables S2-S7, SI). From the differences between the moments of inertia of the parent and mono-substituted isotopic species, we determined the positions of the substituted atoms in the principal axis system using Kraitchman's method[33] and the KRA and EVAL programs[34] (Fig. 2 and Table S8), that are consistent with isomer assignment. For isomer 5, no transitions arising from isotopically-enriched water species could be observed due to its weak spectrum.

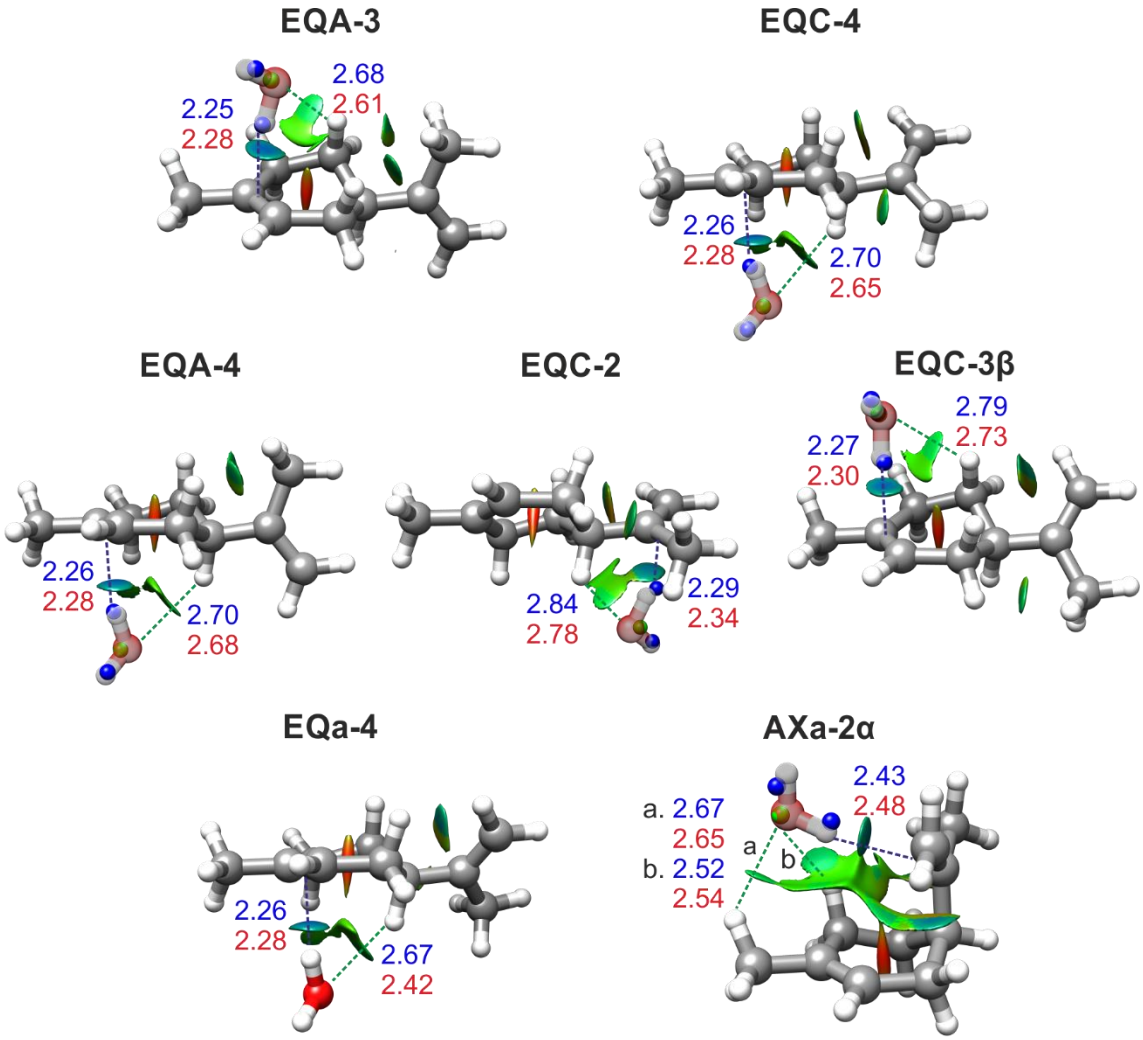

Fig. 2. Overlays of the MP2/6-311++G(d,p) structures of the observed isomers of limonene-H_2O with the r_s positions of the atoms of water from experimental observations (blue spheres). The NCI isosurfaces (s = 0.5) are showed, for values of sign(λ_2)ρ ranging from −0.025 to +0.025 a.u. Blue indicates strong attractive interaction; green indicates weak attractive interaction; and red indicates strong repulsive interaction. The hydrogen bond distances calculated at B3LYP-D3BJ (blue) and MP2 (red) levels of theory are also shown.

The relative abundances of the observed isomers have been estimated considering that they are directly proportional to experimental line intensities and inversely proportional to μ_i^2. The

obtained values are **EQA-3 /EQC-4 / EQA-4 / EQC-2 / EQC-3β / EQa-4 / AXa-2α** = 15 / 11 / 9 / 6 / 4 / 1 / 1. The five most abundant isomers involve limonene in either the EQA or EQC conformation, which are also the most abundant ones for bare limonene.[20]

All isomers identified are low-energy species predicted to be within 4.2 kJ mol^{-1} by both MP2 and B3LYP-D3BJ methods. There are other isomers also predicted to be low in energy that have not been detected, despite repeated and careful searches for them. They may not be sufficiently populated in our experiment, owing to their higher relative energies or lower binding energies, or because they may relax to other lower-energy isomers in the supersonic expansion via low interconversion barriers[35,36] (see SI and Figs. S3-S10).

In all configurations water binds to the double bonds of limonene acting as a hydrogen bond donor and forming O–H···π bonds. C–H···O hydrogen bonds between the oxygen atom of water and the hydrogen atoms of limonene further contribute to the stabilisation of the complexes. We do not observe splittings due to tunneling motions of the hydrogen atoms of water, which can be taken as an indication that water molecules are firmly anchored to limonene.

The binding interactions can be visualised with the aid of the NCI method[37], which determines electron gradient isosurfaces of molecular systems from electron density and its derivatives. The NCI plots of Fig. 2 show light blue isosurfaces indicating attractive O–H···π hydrogen bonds, and green isosurfaces for the weaker attractive C–H···O and dispersion interactions. The latter are present in all isomers, with larger isosurfaces observed for the **AXa-2α** complex, due to the dispersion interactions inherent to axial conformers[20]. Visualisation of the O–H···π hydrogen bonds exposes their differences from stronger hydrogen bonds, such as O–H···O. The latter usually appear as dark blue compact disks along the hydrogen bond[38], showing its strong

attractive character and directionality. In contrast, O–H···π hydrogen bonds are displayed as larger rectangular light-blue isosurfaces, highlighting their lower directionality and weaker attractive nature.

In the majority of the complexes, water interacts with the endocyclic double bond. Only in two complexes, **AXa-2α** and **EQC-2**, water binds to the exocyclic double bond in the isopropenyl substituent. This raises the question of whether the double bonds in limonene have different nucleophilicity. Calculations of the molecular electrostatic potential (MEP) of the observed conformers of bare limonene, at the potential isosurface of 0.001 eau^{-3} (Fig. S11), show that the exocyclic bond is slightly more nucleophilic than the endocyclic bond. Thus the preference of water for endocyclic binding cannot be attributed to the inherent characteristics of the double bonds. Further information about the intermolecular interactions and their relative energies was obtained from Natural Bond Orbital analysis. Our results (Tables S9-S15) confirm that the most stabilising interaction in all isomers is O–H···π hydrogen bonding, with secondary interactions C–H···O and H···O–H_w having varying contributions. O–H···π interactions involving the endocyclic double bond are predicted to be stronger than with the exocyclic one, except in **EQC-3**. Surprisingly, **AXa-2α** has the weakest O–H_w···π hydrogen bonding but the secondary interactions are the strongest and there are many of them, which makes **AXa-2α** the isomer with the largest stabilising intermolecular interactions, followed by **EQA-3**.

The energy ordering, including zero-point corrections, of the predicted isomers differs noticeably between MP2 and B3LYP-D3BJ methods. Both predict the most abundant isomer **EQA-3** as the global minimum, but B3LYP-D3BJ predicts the six lower-energy isomers containing only EQA and EQC limonene conformers while MP2 predicts three of them

containing the AXa limonene conformer. Different predictions from these two methods have been reported for complexes where there are competing non-covalent interactions[38], and for bare molecules where dispersion interactions contribute differently to the stabilisation of different conformations[20,39]. The latter is the case of limonene, which has higher dispersion contributions to axial conformers. Because MP2 tends to overestimate dispersion contributions[38,39], we hypothesise that this is the reason for the higher number of lower-energy complexes involving axial limonene predicted by MP2. The interaction energies, calculated after correcting for Basis Set Superposition Error (BSSE)[40], and using Symmetry Adapted Perturbation Theory (SAPT)[41], also show great variations between MP2 and B3LYP-D3BJ (Tables 1 and S1), with no agreement on the isomer with the largest interaction energy.

Despite the differences in predicting relative and interaction energies, both B3LYP-D3BJ and MP2 methods with the 6-311++G(d,p) basis set yield good predictions of the rotational constants for all observed isomers (see Tables 1 and 2), with average deviations of 1.3% (B3LYP-D3BJ) and 1.6% (MP2) from the experimental rotational constants. We should note that we are comparing equilibrium rotational constants A_e, B_e, C_e (from theory) with ground-state rotational constants A_0, B_0, C_0 (from experiment), which is not strictly correct but it is common practice in the field. B3LYP-D3BJ predicts slightly shorter O–H···π hydrogen bond lengths (2.25 - 2.29 Å) than MP2 (2.28 - 2.34 Å), and slightly longer C–H···O lengths (2.67 - 2.85 Å for B3LYP-D3BJ and 2.42 - 2.78 Å for MP2), see Fig. 2. The **AXa-2α** isomer, where limonene is in an axial conformation, is an outlier in both methods, with O–H···π hydrogen bond lengths of 2.43 Å for B3LYP-D3BJ and 2.48 Å for MP2, and C–H···O interactions involving two different C–H bonds with lengths of 2.52 and 2.67 Å for B3LYP-D3BJ and 2.54 and 2.65 Å for MP2.

The theoretical bond lengths can be compared with those obtained for other molecular systems bound by O–H···π hydrogen bonds. Interestingly, there is not a great wealth of data on O–H···π interactions involving a double bond. For the prototypical system ethylene-H_2O[42], an O–H···π hydrogen bond length of 2.482 Å was derived by adjusting the equilibrium structure until the value of *B*+*C* matched the experimental one. This value is considerably longer than those predicted for limonene-H_2O. A more suitable comparison can be established with cyclopentene-H_2O[43], with reported semi-experimental equilibrium bond lengths of 2.33 Å for O–H···π and 2.79 Å for C–H···O interactions. In the same paper, cyclohexene-H_2O (not studied experimentally) was predicted to have O–H···π and C–H···O bond lengths of 2.31 Å and 2.75 Å, respectively, from B2LYP-D3BJ/maug-cc-pVTZ-dH calculations. The values for the limonene-water isomers are similar to these, with generally shorter values for the C–H···O interactions.

The higher level SAPT calculations[41] (Table S16) run for the observed limonene-H_2O isomers show that electrostatic interactions make the largest contribution (*ca*. 52% on average) to attractive forces, followed by dispersion (*ca*. 28% on average). The relative contributions from electrostatic, exchange, induction and dispersion contributions are comparable to those reported for cyclohexene-water[43]. The overall binding energies are also comparable. In contrast, water complexes involving aromatic molecules such as benzene, acenaphthene and corannulene show significantly larger contributions from dispersion (ranging from 44% in benzene to 59% in corannulene), reflecting the different chemical nature of the intermolecular interaction.

The diversity and number of low-energy isomers observed for limonene-H_2O is remarkable, and shows the ability of water to interact with limonene and its adaptability. The dynamic behaviour of water can influence atmospheric processes, as water may compete for limonene

binding with atmospheric oxidants and steer reactions to follow different paths. For example, one of the important oxidation pathways of limonene in the atmosphere is by reacting with ozone. Ozone reacts much faster (about 30 times) in the gas phase with the endocyclic double bond of limonene than with the exocyclic bond, with products affected by ozone:limonene relative concentrations and relative humidity[5,6,44]. Our observations of a strong preference of water to interact with the endocyclic double bond of limonene point to a possible influence of water before ozonolysis takes place, by effectively competing with ozone. Relative humidity has also been found to affect the ozonolysis of the SOA precursors α- and β-pinene but no effect was observed in reactions involving OH and NO_3 radicals, which can proceed without involving the monoterpene double bond[7]. Our results, showing that water preferentially binds to the endocyclic double bond of limonene and informing on its various arrangements, enrich our knowledge of the possible interactions of limonene in the atmosphere and serve as a stepping stone for further investigations on limonene-water interactions. They may also stimulate more studies on atmospheric reaction rates and mechanisms including water.

Supporting Information. Experimental methods, computational methods, lists of rotational transitions, and details of spectroscopic analyses.

Corresponding Author. *E-mail: maria.sanz@kcl.ac.uk. Tel: +44(0)2078487509.

ORCID:

Isabel Peña: 0000−0001−5336−3217

Maria Eugenia Sanz: 0000-0001-7531-0140.

Notes

The authors declare no competing financial interests.

ACKNOWLEDGMENT

The authors would like to thank funding from the EU FP7 (Marie Curie grant PCIG12-GA-2012-334525) as well as King's College London, and acknowledge use of the research computing facility at King's College London, *Rosalind* (https://rosalind.kcl.ac.uk).

REFERENCES

(1) Kroll, J. H.; Seinfeld, J. H. Chemistry of Secondary Organic Aerosol: Formation and Evolution of Low-Volatility Organics in the Atmosphere. *Atmos. Environ.* **2008**, *42*, 3593–3624.

(2) Boucher, O.; Randall, D.; Artaxo, P.; Bretherton, C.; Feingold, G.; Forster, P.; Kerminen, V.-M.; Kondo, Y.; Liao, H.; Lohmann, U. et al. Clouds and Aerosols. In *Climate Change 2013 - The Physical Science Basis. Working Group I Contribution to the Fifth Assessment Report of the Intergovernmental Panel on Climate Change.*; Intergovernmental Panel on Climate Change, Ed.; Cambridge University Press: Cambridge, 2014; pp 571–658.

(3) Hallquist, M.; Wenger, J. C.; Baltensperger, U.; Rudich, Y.; Simpson, D.; Claeys, M.; Dommen, J.; Donahue, N. M.; George, C.; Goldstein, A. H. et al. The Formation, Properties and Impact of Secondary Organic Aerosol: Current and Emerging Issues. *Atmos. Chem. Phys.* **2009**, *9*, 5155–5236.

(4) Nguyen, T. B.; Roach, P. J.; Laskin, J.; Laskin, A.; Nizkorodov, S. A. Effect of Humidity on the Composition of Isoprene Photooxidation Secondary Organic Aerosol. *Atmos. Chem. Phys.* **2011**, *11*, 6931–6944.

(5) Jonsson, Å. M.; Hallquist, M.; Ljungström, E. Impact of Humidity on the Ozone Initiated Oxidation of Limonene, Δ3-Carene, and α-Pinene. *Environ. Sci. Technol.* **2006**, *40*, 188–194.

(6) Bonn, B.; Schuster, G.; Moortgat, G. K. Influence of Water Vapor on the Process of New Particle Formation during Monoterpene Ozonolysis. *J. Phys. Chem. A* **2002**, *106*, 2869–2881.

(7) Bonn, B.; Moortgat, G. K. New Particle Formation during α- and β-Pinene Oxidation by O3, OH and NO3, and the Influence of Water Vapour: Particle Size Distribution Studies. *Atmos. Chem. Phys.* **2002**, *2*, 83–196.

(8) Vaida, V. Perspective: Water Cluster Mediated Atmospheric Chemistry. *J. Chem. Phys.* **2011**, *135*, 020901.

(9) Schnitzler, E. G.; Badran, C.; Jäger, W. Contrasting Effects of Water on the Barriers to Decarboxylation of Two Oxalic Acid Monohydrates: A Combined Rotational Spectroscopic and Ab Initio Study. *J. Phys. Chem. Lett.* **2016**, *7*, 1143–1147.

(10) Kanakidou, M.; Seinfeld, J. H.; Pandis, S. N.; Barnes, I.; Dentener, F. J.; Facchini, M. C.; Van Dingenen, R.; Ervens, B.; Nenes, A.; Nielsen, C. J. et al. Organic Aerosol and Global Climate Modelling: A Review. *Atmos. Chem. Phys.* **2005**, *5*, 1053–1123.

(11) Boyd, C. M.; Nah, T.; Xu, L.; Berkemeier, T.; Ng, N. L. Secondary Organic Aerosol

(SOA) from Nitrate Radical Oxidation of Monoterpenes: Effects of Temperature, Dilution, and Humidity on Aerosol Formation, Mixing, and Evaporation. *Environ. Sci. Technol.* **2017**, *51*, 7831−7841.

(12) Cabezas, C.; Nakajima, M.; Endo, Y. Criegee Intermediates Meet Rotational Spectroscopy. *Int. Rev. Phys. Chem.* **2020**, *39*, 349–382.

(13) Pérez, C.; Krin, A.; Steber, A. L.; López, J. C.; Kisiel, Z.; Schnell, M. Wetting Camphor: Multi-Isotopic Substitution Identifies the Complementary Roles of Hydrogen Bonding and Dispersive Forces. *J. Phys. Chem. Lett.* **2016**, *7*, 154–160.

(14) Chrayteh, M.; Huet, T. R.; Dréan, P. Microsolvation of Myrtenal Studied by Microwave Spectroscopy Highlights the Role of Quasi-Hydrogen Bonds in the Stabilization of Its Hydrates. *J. Chem. Phys.* **2020**, *153*, 104304.

(15) Chrayteh, M.; Savoia, A.; Huet, T. R.; Dréan, P. Microhydration of Verbenone: How the Chain of Water Molecules Adapts Its Structure to the Host Molecule. *Phys. Chem. Chem. Phys.* **2020**, *22*, 5855–5864.

(16) Chrayteh, M.; Huet, T. R.; Dréan, P. Gas-Phase Hydration of Perillaldehyde Investigated by Microwave Spectroscopy Assisted by Computational Chemistry. *J. Phys. Chem. A* **2020**, *124*, 6511–6520.

(17) Blanco, S.; López, J. C.; Maris, A. Terpenoids: Shape and Non-Covalent Interactions. The Rotational Spectrum of: Cis -Verbenol and Its 1 : 1 Water Complex. *Phys. Chem. Chem. Phys.* **2020**, *22*, 5729–5734.

(18) Partal Ureña, F.; Moreno, J. R. A.; López González, J. J. Conformational Study of (R)-

(+)-Limonene in the Liquid Phase Using Vibrational Spectroscopy (IR, Raman, and VCD) and DFT Calculations. *Tetrahedron: Asymmetry* **2009**, *20*, 89–97.

(19) Reinscheid, F.; Reinscheid, U. M. Stereochemical Analysis of (+)-Limonene Using Theoretical and Experimental NMR and Chiroptical Data. *J. Mol. Struct.* **2016**, *1106*, 141–153.

(20) Loru, D.; Vigorito, A.; Santos, A. F. M.; Tang, J.; Sanz, M. E. The Axial/Equatorial Conformational Landscape and Intramolecular Dispersion: New Insights from the Rotational Spectra of Monoterpenoids. *Phys. Chem. Chem. Phys.* **2019**, *21*, 26111–26116.

(21) Moreno, J. R. A.; Huet, T. R.; González, J. J. L. Conformational Relaxation of S-(+)-Carvone and R-(+)-Limonene Studied by Microwave Fourier Transform Spectroscopy and Quantum Chemical Calculations. *Struct. Chem.* **2013**, *24*, 1163–1170.

(22) Grimme, S.; Ehrlich, S.; Goerigk, L. Effect of the Damping Function in Dispersion Corrected Density Functional Theory. *J. Comput. Chem.* **2011**, *32*, 1456–1465.

(23) Grimme, S.; Antony, J.; Ehrlich, S.; Krieg, H. A Consistent and Accurate Ab Initio Parametrization of Density Functional Dispersion Correction (DFT-D) for the 94 Elements H-Pu. *J. Chem. Phys.* **2010**, *132*, 154104.

(24) Frisch, M. J.; Trucks, G. W.; Schlegel, H. B.; Scuseria, G. E.; Robb, M. A.; Cheeseman, J. R.; Scalmani, G.; Barone, V.; Mennucci, B.; Petersson, G. A. et al. *Gaussian 09, Revision E. 01; Gaussian*; 2009.

(25) Loru, D.; Bermúdez, M. A.; Sanz, M. E. Structure of Fenchone by Broadband Rotational Spectroscopy. *J. Chem. Phys.* **2016**, *145*, 074311.

(26) Loru, D.; Peña, I.; Sanz, M. E. Ethanol Dimer: Observation of Three New Conformers by Broadband Rotational Spectroscopy. *J. Mol. Spectrosc.* **2017**, *335*, 93–101.

(27) Pérez, C.; Muckle, M. T.; Zaleski, D. P.; Seifert, N. A.; Temelso, B.; Shields, G. C.; Kisiel, Z.; Pate, B. H. Structures of Cage, Prism, and Book Isomers of Water Hexamer from Broadband Rotational Spectroscopy. *Science (80-.).* **2012**, *336*, 897–902.

(28) Richardson, J. O.; Pérez, C.; Lobsiger, S.; Reid, A. A.; Temelso, B.; Shields, G. C.; Kisiel, Z.; Wales, D. J.; Pate, B. H.; Althorpe, S. C. Concerted Hydrogen-Bond Breaking by Quantum Tunneling in the Water Hexamer Prism. *Science (80-.).* **2016**, *351*, 1310–1313.

(29) Pérez, C.; Lobsiger, S.; Seifert, N. A.; Zaleski, D. P.; Temelso, B.; Shields, G. C.; Kisiel, Z.; Pate, B. H. Broadband Fourier Transform Rotational Spectroscopy for Structure Determination: The Water Heptamer. *Chem. Phys. Lett.* **2013**, *571*, 1–15.

(30) Pérez, C.; Zaleski, D. P.; Seifert, N. A.; Temelso, B.; Shields, G. C.; Kisiel, Z.; Pate, B. H. Hydrogen Bond Cooperativity and the Three-Dimensional Structures of Water Nonamers and Decamers. *Angew. Chemie - Int. Ed.* **2014**, *53*, 14368–14372.

(31) Watson, J. K. G. Aspects of Quartic and Sextic Centrifugal Effects on Rotational Energy Levels. In *Vibrational spectra and structure, vol.6. A series of advances*; Durig, J. R., Ed.; 1977; pp 1–89.

(32) Pickett, H. M. The Fitting and Prediction of Vibration-Rotation Spectra with Spin Interactions. *J. Mol. Spectrosc.* **1991**, *148*, 371–377.

(33) Kraitchman, J. Determination of Molecular Structure from Microwave Spectroscopic Data. *Am. J. Phys.* **1953**, *21*, 17–24.

(34) Kisiel, Z. PROSPE-Programs for Rotational Spectroscopy. *Spectrosc. from Sp.* **2001**, 91–106.

(35) Ruoff, R. S.; Klots, T. D.; Emilsson, T.; Gutowsky, H. S. Relaxation of Conformers and Isomers in Seeded Supersonic Jets of Inert Gases. *J. Chem. Phys.* **1990**, *93*, 3142–3150.

(36) Erlekam, U.; Frankowski, M.; Von Helden, G.; Meijer, G. Cold Collisions Catalyse Conformational Conversion. *Phys. Chem. Chem. Phys.* **2007**, *9*, 3786–3789.

(37) Chaudret, R.; De Courcy, B.; Contreras-García, J.; Gloaguen, E.; Zehnacker-Rentien, A.; Mons, M.; Piquemal, J. P. Unraveling Non-Covalent Interactions within Flexible Biomolecules: From Electron Density Topology to Gas Phase Spectroscopy. *Phys. Chem. Chem. Phys.* **2014**, *16*, 9876–9891.

(38) Burevschi, E.; Alonso, E. R.; Sanz, M. E. Binding Site Switch by Dispersion Interactions: Rotational Signatures of Fenchone-Phenol and Fenchone-Benzene Complexes. *Chem. Eur. J.* **2020**, *26*, 11327 –11333.

(39) Uriarte, I.; Insausti, A.; Cocinero, E. J.; Jabri, A.; Kleiner, I.; Mouhib, H.; Alkorta, I. Competing Dispersive Interactions: From Small Energy Differences to Large Structural Effects in Methyl Jasmonate and Zingerone. *J. Phys. Chem. Lett.* **2018**, *9*, 5906–5914.

(40) Boys, S. F.; Bernardi, F. The Calculation of Small Molecular Interactions by the Differences of Separate Total Energies. Some Procedures with Reduced Errors. *Mol. Phys.* **1970**, *19*, 553–566.

(41) Misquitta, A. J.; Podeszwa, R.; Jeziorski, B.; Szalewicz, K. Intermolecular Potentials Based on Symmetry-Adapted Perturbation Theory with Dispersion Energies from Time-

Dependent Density-Functional Calculations. *J. Chem. Phys.* **2005**, *123*, 214103.

(42) Peterson, K. I.; Klemperer, W. Water-Hydrocarbon Interactions: Structure and Internal Rotation of the Water-Ethylene Complex. *J. Chem. Phys.* **1986**, *85*, 725–732.

(43) Wang, J.; Spada, L.; Chen, J.; Gao, S.; Alessandrini, S.; Feng, G.; Puzzarini, C.; Gou, Q.; Grabow, J.-U.; Barone, V. The Unexplored World of Cycloalkene-Water Complexes: Primary and Assisting Interactions Unraveled by Experimental and Computational Spectroscopy. *Angew. Chemie Int. Ed.* **2019**, *58*, 13935 –13941.

(44) Maksymiuk, C. S.; Gayahtri, C.; Gil, R. R.; Donahue, N. M. Secondary Organic Aerosol Formation from Multiphase Oxidation of Limonene by Ozone: Mechanistic Constraints via Two-Dimensional Heteronuclear NMR Spectroscopy. *Phys. Chem. Chem. Phys.* **2009**, *11*, 7810–7818.